Materiales de Construcción
Vol. 73, Issue 352, October-December 2023, e329
ISSN-L: 0465-2746
https://doi.org/10.3989/mc.2023.352223

Experimental investigation of the behavior of concrete beams containing recycled materials reinforced with composite rebars

R. Jafari[a], M.H. Alizadeh-Elizei[a]✉, M. Ziaei[b], R. Esmaeil-Abadi[a]

a. Department of Civil Engineering, Roudehen Branch, Islamic Azad University, (Roudehen, Iran)
b. Department of Civil Engineering, Faculty of Engineering, Garmsar University, (Garmsar, Iran)
✉: alizadeh.elizei@iau.ac.ir

Received 31 March 2023
Accepted 30 August 2023
Available on line 1 December 2023

ABSTRACT: The application of various Fiber Reinforced Polymer (FRP) composite materials is very widespread in the world. The use of recycled materials in concrete, can improve some of the mechanical properties of concrete. In this laboratory research, the behavior of reinforced concrete beams with composite rebars with glass fibers made of concrete containing recycled materials such as glass, rubber and micro-silica with different mixing plans has been investigated. These mixing plans are such that recycled glass and rubber aggregates have replaced a percentage of fine and coarse concrete aggregates, and glass powder and micro-silica have also replaced a percentage of concrete cement. The results showed that the replacement of coarse rubber, glass powder, and micro-silica in concrete materials increases the bending strength and ductility of concrete beam. In examining the microstructure of concrete by Scanning Electron Microscope (SEM) the adhesiveness of the rubber Interfacial Transition Zone (ITZ) in concrete was suitable.

KEY WORDS: Composite rebar; Glass; Rubber; Recycled materials; Micro-silica.

Citation/Citar como: Jafari, R.; Alizadeh Elizei, M.H.; Ziaei, M.; Esmaeil Abadi, R. (2023) Experimental investigation of the behavior of concrete beams containing recycled materials reinforced with composite rebars. Mater. Construcc. 73 [352], e329. https://doi.org/10.3989/mc.2023.352223.

RESUMEN: *Investigación experimental del comportamiento de vigas de hormigón con materiales reciclados y armadas con varillas corrugadas hechas con material compuesto.* Los materiales compuestos reforzados con fibras poliméricas (FRP por sus siglas en inglés) son de uso muy extendido en el mundo. El uso de materiales reciclados en el hormigón puede mejorar algunas de sus propiedades mecánicas. En esta investigación experimental se ha estudiado el comportamiento de vigas armadas con varillas corrugadas hechas de materiales compuestos con fibras de vidrio; dichas vigas se fabricaron con hormigón con materiales reciclados teles como vidrio, goma y humo de sílice, empleando distintos diseños de mezcla. En estos diseños de mezcla, los áridos de vidrio reciclado y goma reemplazan a cierto porcentaje de áridos finos y gruesos del hormigón y, el polvo de vidrio y humo de sílice sustituyen a cierto porcentaje del cemento del hormigón. Los resultados indican que la sustitución de áridos de goma gruesos, polvo de vidrio y humo de sílice en los materiales de hormigón, redunda en un incremento en resistencia a la flexión y ductilidad de la viga de hormigón. En el examen microscópico de la microestructura del hormigón mediante microscopía electrónica de barrido (SEM), se observó un nivel adecuado de adhesión en la zona de transición interfacial (ITZ) de goma en el hormigón.

PALABRAS CLAVE: Armadura compuesta; Vidrio; Goma; Materiales reciclados; Humo de sílice.

1. INTRODUCTION

Fiber Reinforced Polymer (FRP) materials are used in the construction industry as relatively new materials for purposes such as new construction, retrofitting, or seismic improvement (1-4). FRP or composite rebars are produced from the combination of fibers and a matrix (resin coating) and have many advantages, including high tensile strength, light weight, corrosion resistance, insulation in magnetic and electric fields, and easy application such as convenient transportation, cutting and installation. The weak points of these rebars are their sensitivity to heat and low shear strength. Among the types of FRP rebars, Glass Fiber Reinforced Polymer (GFRP) rebars are considered the most widely used and consumed. Sand-blasted Glass Fiber Reinforced Polymer (SGFRP) rebar is the same GFRP rebar that is coated with sand during production. This work can increase the adhesion strength of rebar to concrete.

On the other hand, due to their large volume, waste materials have become a big problem worldwide, and the reuse of these recycled materials in the construction industry can help to solve this problem (5-7). The use of waste materials such as micro-silica, glass, and rubber in concrete is one of the practical methods of reusing these materials, which improves some of the mechanical and dynamic properties of concrete and is effective in changing its performance (8-12). In the following, the use of recycled materials in reinforced concrete with FRP and steel rebars has been investigated.

Many researchers have used FRP rebars as an alternative to traditional steel rebars in reinforced concrete members subjected to uniform and cyclic loading (13). Using these products mutually and continuously will lead to a sustainable and economical construction system (14). A number of researchers have investigated the behavior of beams reinforced with FRP bars and made of normal strength concrete (NSC) or high-strength concrete (HSC) and different concretes under flexural loading (15-22). Hama *et al.* (23) have investigated the effect of using waste glass powder as a substitute for cement weight percentages with values of 0% (reference), 10%, and 15%, as well as the structural behavior of reinforced concrete beams containing waste glass powder. In this research, concrete beams (width 150 mm, height 150 mm and span length 900 mm) were used. The results showed that the beams containing waste glass powder showed good strength and satisfactory bending performance compared to the reference beams. Eisa *et al*. (24) investigated the effect of the combination of waste crumb rubber ranging in size between 2 and 3 mm and hooked-end steel fibers with a diameter of 0.80 mm and length of 50 mm with a tensile strength of 1000 MPa and elastic modulus of 210 GPa on the behavior of reinforced concrete beams under static loads by four-point bending test. Crumb rubber with different weight percentages (5%, 10%, 15%, and 20%) has been a partial replacement of fine aggregates in the mixture of normal concrete and concrete containing steel fibers. The volume amount of steel fibers is kept constant at 1%. The test results showed that the use of crumb rubber as a relative substitute of fine aggregates at the rate of 5% and 10% shows an acceptable performance of reinforced concrete beams. The use of steel fibers with rubber concrete with a rubber percentage of more than 10% improved the performance and toughness of these mixtures. Shahjalal *et al*. (25) investigated the combined effect of recycled aggregates, crumb rubber and polypropylene fibers with specific gravity of 0.91 g/cm^3, length of 12 mm, tensile strength of 480 MPa, and elastic modulus of 7 GPa with contents at 0.5% on the physical and mechanical properties of concrete. Fourteen specimens of reinforced concrete beams with dimensions of 150×200×1500 (mm) were made and tested. Several mixing plans in which the variables included 5% and 10% crumb rubber and steel ratio 0.59% and 1.60% and recycled coarse aggregates and polypropylene fibers were kept constant at 30% and 0.5%, respectively. The results of the experimental study show the improvement of short-term and long-term mechanical properties of concretes containing crumb rubber and polypropylene fibers. Concrete beams with 30% recycled coarse aggregates, 5% crumb rubber, and 0.5% polypropylene fibers improved bending capacity, ductility and toughness. Ismail and Hassan (26) developed twelve concrete beams to investigate the effect of crumb rubber with and without steel fibers on the bending behavior of large-scale beams. The main parameters included the percentage of rubber particles (0-35% of sand volume), the volume of steel fibers (0, 35% and 1%), and the length of steel fibers (35 mm and 60 mm). The results showed that the increase in rubber particles reduces the width of the crack, reduces the weight of the concrete itself and improves the deformation at a given load. For example, the beam with 15% crumb rubber was able to reach an ultimate load, ductility, and toughness of about 90%, 102%, and 91% of the reference beam, respectively. In contrast, the addition of a high percentage of crumb rubber (more than 15%) showed a significant decrease in ductility, toughness, first crack moment and ultimate bending capacity of the tested beams. Erfan *et al*. (27) investigated the bending behavior of concrete beams reinforced with GFRP polymer rebars in mixtures of nano-silica concrete and high-strength concrete. The results show that the breaking and displacement loads of beams reinforced with GFRP rebars have increased by 22% and 6.5 times, respectively, compared to beams with steel rebars and concrete containing nano-silica. Cracks along the length and width of the GFRP beams were also reduced. Also, the first crack force of beams reinforced with GFRP bars shows a reduction of 8.5%

compared to beams with steel bars. De sá *et al*. (28) investigated the behavior of reinforced concrete beam with GFRP rebars and polypropylene macro-fibers. The polypropylene macro-fibers used in this research are 51 mm long with an aspect ratio of 74. A reinforcement ratio of 10 kg/m^3 of polypropylene fiber was used throughout this research, corresponding to a volume fraction of approximately 1%. The modulus of elasticity and tensile strength are respectively 9.5 GPa and 600-650 MPa. The results showed that in structural concrete beams, the addition of polypropylene macro-fibers increased stiffness by about 10% and the concrete ultimate strains by up to 40%. This latter phenomenon led to an increase in ductility up to 162%, which showed that the addition of macro-polypropylene fibers is a suitable strategy in overcoming some of the weaknesses of GFRP reinforced concrete members. Arunbalaji *et al*. (29) investigated the mechanical properties of cement concrete with and without micro-silica and nano-silica particles. The water-cement ratio of concrete mixtures was a constant value of 0.53. The amount of micro-silica replacing cement in this research was 10% and added nano-silica was 0%, 0.5%, 1.0%, and 1.5%. The development of mechanical strength showed that replacing 10% of micro-silica and adding 0.5% of nano-silica was the optimal ratio. El-Mandouh *et al*. (30) investigated the shear strength of sixteen full-scale over-reinforced concrete beams with and without nano-silica made of high-strength concrete in both experimental and analytical ways. Nano-silica was used as a partial replacement for Portland cement. The experimental results showed that increasing the ratio of nano-silica, decreased the number of cracks and increased the distance between cracks while decreasing the crack width. For specimens with stirrups and a Shear span to effective depth ratios of 1.5, raising nano-silica from 0% to 1%, 2%, and 3% increased the ultimate load by 8%, 21%, and 30%, respectively. Additionally, the addition of nano-silica to concrete boosted the contribution of the concrete to the shear strength. Jafari *et al*. (31), in a laboratory study, investigated the replacement of rubber and glass with concrete aggregate and cement. In this study, rubber with two sizes of fine and coarse aggregate with ratios of 5% and 10% and glass powder with ratios of 10%, 15%, and 20% were added together and with different mixing plans in the reference concrete. The results showed that this replacement reduced the compressive strength and increased the tensile strength. In concrete containing 5% coarse rubber (5-10 mm) and 10% glass powder, the compressive strength decreased by 12% and the tensile strength increased by 28% compared to the reference concrete. Also, in concrete containing 5% fine rubber (1-3 mm) and 10% glass powder, the compressive strength has decreased by 30% compared to the reference concrete. The optimal percentage of replacement values were 5% for rubber and 10% for glass.

In this present laboratory research, 13 concrete beams have been made from 10 different mixing plans, and the effect of substituting glass powder and micro-silica instead of cement and glass crumb instead of fine aggregate and crumb rubber instead of fine and coarse aggregate in concrete beams reinforced with GFRP, SGFRP and steel rebars have been investigated. The variables of this research include the type of rebar, the size of replacement rubber, the size of replacement glass and the types of combinations glass, rubber and micro-silica in the beams concrete. According to previous studies (23-27, 29-31, 32, 33), the size of the rubber used in concrete in this research is in two categories: 0 to 5 mm and 5 to 10 mm, which has been replaced by fine and coarse aggregate in the separate mixing plan with a replacement value of 5%. The size of glass powder used in concrete is maximum 75 microns, which is replaced by 10% of cement, and the size of glass crumb used is in the range of 0 to 5 mm, which is replaced by 5% of fine aggregate. The size of micro-silica used in concrete is about 0.05 to 0.2 micron, which is replaced by 10% of cement.

One of the main objectives of this research is to obtain an optimal mixing plan of recycled materials in reinforced concrete beam with GFRP rebars to increase its bending strength and ductility. Investigating the behavior of beams reinforced with GFRP rebars containing recycled materials in concrete is one of the other objectives. On the other hand, concrete made with recycled materials can help the environment due to the use of recycled materials while reducing the cost of making concrete by using less raw materials in building constructions.

2. EXPERIMENTAL PROGRAM

The experimental program in this research includes the construction of three groups of reinforced concrete beams with GFRP, SGFRP composite rebars and steel rebars, from 10 different mixing plans.

2.1. Material specifications

2.1.1. Aggregates (sand and gravel)

The aggregates used in concrete should be in such a way that they can be used to make concrete with sufficient strength, durability in aggressive environmental conditions, suitable consistency and workability (34). Besides, aggregate skeleton is essential for having volumetric stability.

The fine aggregate (sand) used is broken type, with a maximum size of 4.75 mm. The test of specific gravity and water absorption of fine aggregate materials has been carried out according to ASTM C128 (35). The specific gravity SSD of sand

is 2.56 g/cm^3 and its apparent specific gravity is 1.65 g/cm^3 and its water absorption is 2.83% and also the fineness modulus of sand is 3.25.

The coarse aggregate (gravel) used with the largest nominal size is 19 mm for gravel 3/4" and 9.5 mm for gravel 3/8". The test of specific gravity and water absorption of coarse aggregate materials has been carried out according to ASTM C127 (36). The specific gravity SSD of 3/4" and 3/8" gravel is 2.58 g/cm^3 and 2.57 g/cm^3, their apparent specific gravity is 1.62 g/cm^3 and 1.61 g/cm^3, their water absorption is 1.56% and 1.83% have been obtained, respectively. The ratio of fine aggregate to coarse aggregate was 1.25 to 1 by weight. The granulation curve of sand and gravel used in concrete is presented in Figure 1.

2.1.2. Cement

The cement used in this experiment is Portland cement type 2 or modified Portland cement. This cement has a specific weight of 3.15 g/cm^3 and a specific surface area of 3150 cm^2/g and an autoclave expansion of 0.046 and a compressive strength in 28 days of 440 kg/cm^2 and satisfies all the requirements of ASTM C150 (37). The chemical characteristics of cement are given in Table 1.

2.1.3. Rubber

Rubber are different in terms of ingredients, especially due to the amount of natural and synthetic rubber in them (38). The crumb rubber was prepared from the mechanical grinding of waste truck tires without

Table 1. Chemical characteristics of Type 2 cement.

Composition	Result (%)	Factory standard	ASTM C150
SiO_2	21.11	Min 20.5	-
Al_2O_3	4.48	Max 5	Max 6
Fe_2O_3	3.91	Max 5	Max 6
CaO	63.36	-	-
MgO	1.48	Max 2.5	Max 6
SO_3	2.58	Max 2.9	Max 3
Na_2O	0.43	-	-
K_2O	0.48	-	-
Loss on Ignition	2.25	Max 2.9	Max 3
Insoluble Residue	0.45	Max 0.7	Max 1.5
F.CaO	1.50	-	-
C_3S	52.8	-	-
C_2S	21.0	-	-
C_3A	5.3	-	Max 8

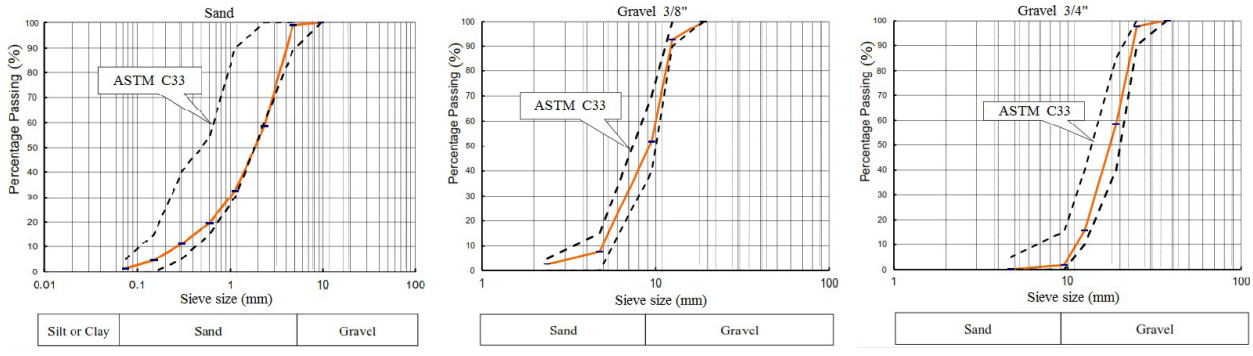

Figure 1. Granulation curve of sand and gravel.

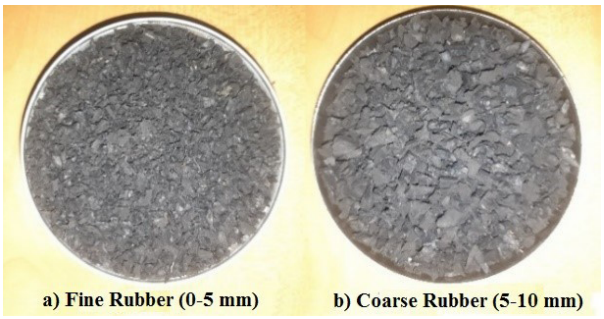

Figure 2. Rubber particles used in concrete.

any pollution or modification. As shown in Figure 2, the crumb rubber had two size categories: 0-5 mm and 5-10 mm with a specific weight of 1.05 g/cm^3. These were used as a substitute for part of the fine and coarse aggregates. Water absorption of both size categories of rubber particles is considered insignificant. The chemical characteristics of rubber particles used in the research are given in Table 2.

2.1.4. Glass

Glass can be used in concrete in three ways: coarse aggregate, fine aggregate and glass powder, each of which can have different reactions with the composition of concrete and lead to a significant effect on the quality of concrete obtained (39). In this experiment, recycled glass obtained from building glass was used, which does not contain impurities and other types of glass, such as bottle glass, lamps, etc. As shown in Figure 3, glass powder and glass crumb are used in this research. The specifics of these two groups are as follows; glass powder maximum size are 75 microns (passing a 200 grade sieve) with a specific surface area of 2618 cm^2/g and a specific weight of 2.94 g/cm^2, while the glass crumb are 0-5 mm in size, with the same grain size as sand. Glass powder has been used as a part of cement and glass crumb have been used as a part of fine aggregate of concrete. The chemical characteristics of the glass used in the research are shown in Table 3.

Table 2. Chemical composition of recycled crumb rubber.

Chemical composition	Percentage (%)
Styrene Butadiene Rubber (SBR)	49.0
Carbon Black	46.0
Extender Oil	1.8
Zinc Oxide	1.2
Stearic Acid	0.5
Sulphur	0.8
Accelerator	0.7

Table 3. Chemical composition of the glass used.

Composition	Result(%)	Heavy metal		
SiO_2	71.5	Analysis	Limit	Test
Al_2O_3	0.7		(ppm)	
Na_2O	13.3	Lead	200	25
Fe_2O_3	0.4	Cadmium	200	-
CaO	7.6	Mercury	200	-
MgO	5.5	Hexavalent Chromium (Cr^{6+})	200	-
K_2O	<0.01	Arsenic	200	34
TiO_2	<0.01	Antimony	200	-
Loss on Ignition	1	Barium	200	25

Figure 3. Glass powder and glass crumb used to in research.

2.1.5. Micro-silica

The size of micro-silica particles is about 0.05 to 0.2 microns. This material has a non-crystalline molecular structure (amorphous) and has a specific surface area of 2×10^5 cm^2/g and an average bulk density of 0.65 g/cm^3 and a specific density of 2.2. The specifications of micro-silica comply with ASTM C1240 Standard (40). The chemical specifications of micro-silica are shown in Table (4).

2.1.6. Rebars

The longitudinal rebars used in the experiment are GFRP, SGFRP and steel, all with a diameter of 10 mm. The composite rebars made by pultrusion method and steel rebar are shown in Figure 4. The stirrup rebars used in all the beams are of steel type and have a diameter of 8 mm. The mechanical characteristics of rebars are given in Table 5.

Table 4. Chemical characteristics of micro-silica.

Composition	Result (%)	ASTMC1240	INSO13278
SiO_2	90-95	Min, 85%	Min 85%
Fe_2O_3	0.4-2	-	-
CaO	2-2.3	-	-
Al_2O_3	2-2.3	-	-
MgO	0.1-0.9	-	-
Moisture Content	0.5	Max, 3%	Max, 3%
Loss on Ignition	4	Max, 6%	Max, 6%

Table 5. Mechanical properties of reinforcing GFRP, SGFRP and steel rebars.

Material properties	GFRP rebar	SGFRP rebar	Steel rebar
Ultimate Strength (MPa)	700	700	400
Tension Modulus of Elasticity (GPa)	55	55	200
Rupture Strain (%)	1.5	1.5	10
Elongation (%)	2.2	2.2	25
Rebar diameter (mm)	10	10	10

Figure 4. Composite rebars (GFRPS, GFRP) and steel rebar.

2.2. Concrete mixing plans

A concrete mixing plan was designed according to ACI-211.1-91 standard (41) as a reference concrete with a cement amount of 425 kg/m^3 and a water-cement ratio of 0.41. Then glass, rubber and micro-silica were replaced in the reference concrete according to 10 plans and with specific percentages.

The replacement method is that in mixing plans containing glass powder, first, 10% is reduced from the cement of the reference concrete mixing plan and the same amount of glass powder is added. In mixing plans containing glass crumb, first, 5% is reduced from the fine aggregate (sand) of the reference concrete mixing plan and the same amount of glass crumb are added. In mixing plans containing micro-silica, first, 10% by weight is reduced from the cement of the reference concrete mixing plan, and the volumetric equivalent of micro-silica is added. The replacement in mixing plans containing fine rubber is that first, 5% is reduced from the fine aggregate (sand) of the reference concrete mixing plan, and fine rubber is added to the same volume ratio. In mixing plans containing coarse rubber, first of the coarse aggregate (3/8" and 3/4" gravel) of the reference concrete mixing plan, according to their ratio, 5% is reduced and coarse rubber is added to the same volume ratio.

The mixing plans are named as follows: P (glass Powder), B (glass crumb), F (Fine rubber) (0-5 mm), C (Coarse rubber) (5-10 mm) and M (Micro-silica) and the number after it indicates the percentage of using this material as a substitute in concrete. For example, the P10F5 plan represents the amount of 10% glass powder instead of cement and 5% fine rubber 0 to 5 mm instead of fine aggregate concrete in the reference plan, or the P10C5M10 plan represents the amount of 10% glass powder instead of cement and 5% coarse rubber 5 to 10 mm instead of coarse aggregate and 10% micro-silica replaces cement again. In Table 6, the materials and specifications of the mixing plans are stated.

2.3. Specifications of beams

The initial plan of concrete beams with FRP and steel rebars were done according to ACI440.1R-15 (42) and ACI 318-19 (43) standards, respectively. 13 concrete beams with dimensions of 650×150×150 mm^3 (width 150 mm, height 150 mm and length 650 mm) are reinforced with three groups of GFRP, SGFRP and steel rebars, and their concretes are made from 10 different mixing plans, including normal concrete and concretes contain rubber, glass and micro-silica. Beams are named as B-GF (Beams reinforced with GFRP rebars), B-SGF (Beams reinforced with SGFRP rebars) and B-St (Beams reinforced with steel rebars). The number after them indicates the type of concrete. The specifications of the beams and their type of concrete are stated in Table 7 and in Figure 5. The supports of all concrete beams are designed to simulate simply supported beam conditions where both ends are free to rotate about an axis perpendicular to the length of the beam. Figure 5 shows the geometric details and dimensions of the designed beams.

2.4. Making concrete specimens

The construction and molding of the studied concrete specimens were done according to ASTM C192 (44) and ASTM C172 (45) standards. Specimens were cured according to ASTM C511 (46) standard for 28 days. To make concrete specimens, first, gravel and part of water are poured into the mixer. The mixer is turned on and sand and rubber (if any), cement, micro-silica (if any) and glass powder (if any) and the rest of the water are added. Mixing and addition of Superplasticizer continues according to schedule. The concrete made in the mixer is poured into the mold and the vibration stage is done with a vibrating table. After 24 hours, the specimens are removed from the mold and placed in the curing tank for 28 days. After that, the specimens are removed from the curing tank and the desired tests are performed on them. Due to the fact that the addition of rubber, glass and micro-silica reduces the workability of concrete, Superplasticizer has been used to obtain a suitable slump for concrete molding. Part of the steps of making the specimens is shown in Figure 6.

3. TESTS AND RESULTS

Slump test on fresh concrete, compressive strength and bending strength tests and scanning electron microscope (SEM) images have been performed on the specimens.

Table 6. Details of the mixing plans used in the research.

Plan Symbol	Type of Glass replaced	Glass (%)	Type of Rubber replaced	Rubber (%)	Micro-silica (%)	Fine	Coarse (Gravel)		Cement 3/4”	Glass Powder	Glass Crumb	Rubber	Micro-silica	Water	* SP	** SP/C (%)
							Sand	3/8”								
						Kg/m^3										
Reference	-	0	-	0	0	958	253	509	425	0	0	0	0	175	0	0
P10F5	Powder	10	Fine	5	0	910	253	509	382.5	42.5	0	19.5	0	175	0.62	0.14
P10C5	Powder	10	Coarse	5	0	958	240	484	382.5	42.5	0	15.5	0	175	0.62	0.14
P10B5	Powder& Crumb	10& 5	-	0	0	910	253	509	382.5	42.5	48	0	0	175	0.62	0.14
P10F5M10	Powder	10	Fine	5	10	910	253	509	340	42.5	0	19.5	30	175	1.00	0.23
P10C5M10	Powder	10	Coarse	5	10	958	240	484	340	42.5	0	15.5	30	175	1.00	0.23
P10B5M10	Powder& Crumb	10& 5	-	0	10	910	253	509	340	42.5	48	0	30	175	1.00	0.23
F5M10	-	0	Fine	5	10	910	253	509	382.5	0	0	19.5	30	175	0.62	0.14
C5M10	-	0	Coarse	5	10	958	240	484	382.5	0	0	15.5	30	175	0.62	0.14
B5M10	Crumb	10	-	0	10	910	253	509	382.5	0	48	0	30	175	0.62	0.14

*Superplasticizer - ** Superplasticizer to cement ratio

Table 7. Details and specifications of the tested beams.

No.	Beams Symbol	Section (mm)	Type of Rebar	Rebars	Stirrups	Concrete Mixing Plans
1	B-GF-1	b150*h150	GFRP	4Φ10mm	Steel-Φ8mm	Reference
2	B-GF-2	b150*h150	GFRP	4Φ10mm	Steel-Φ8mm	P10F5
3	B-GF-3	b150*h150	GFRP	4Φ10mm	Steel-Φ8mm	P10C5
4	B-GF-4	b150*h150	GFRP	4Φ10mm	Steel-Φ8mm	P10B5
5	B-GF-5	b150*h150	GFRP	4Φ10mm	Steel-Φ8mm	P10F5M10
6	B-GF-6	b150*h150	GFRP	4Φ10mm	Steel-Φ8mm	P10C5M10
7	B-GF-7	b150*h150	GFRP	4Φ10mm	Steel-Φ8mm	P10B5M10
8	B-GF-8	b150*h150	GFRP	4Φ10mm	Steel-Φ8mm	F5M10
9	B-GF-9	b150*h150	GFRP	4Φ10mm	Steel-Φ8mm	C5M10
10	B-GF-10	b150*h150	GFRP	4Φ10mm	Steel-Φ8mm	B5M10
11	B-SGF-1	b150*h150	SGFRP	4Φ10mm	Steel-Φ8mm	Reference
12	B-St-1	b150*h150	Steel	4Φ10mm	Steel-Φ8mm	Reference
13	B-SGF-1-2	b150*h150	SGFRP	4Φ10mm	Steel-Φ8mm	Reference

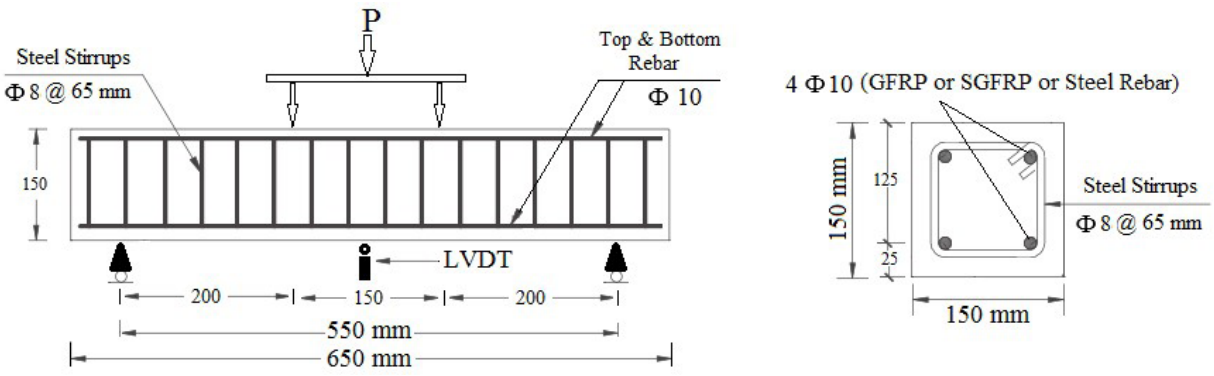

Figure 5. Dimensions and details of reinforced concrete beams.

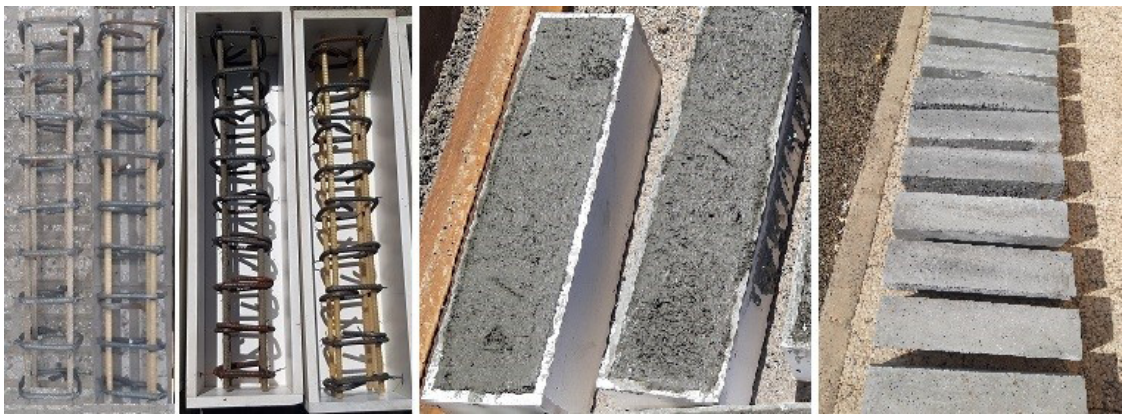

Figure 6. The process of making and molding beam specimens.

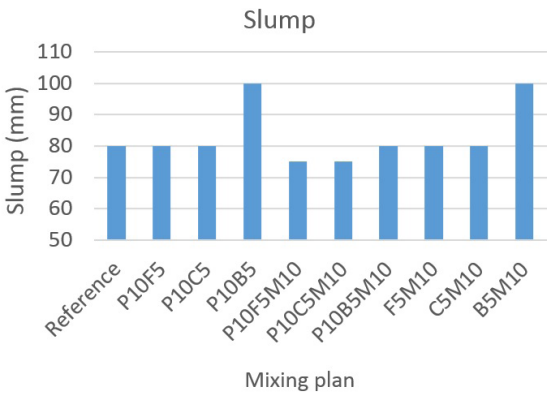

Figure 7. Slump test variations of mixing plans.

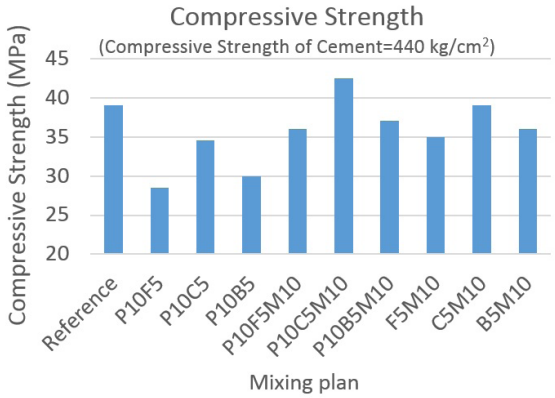

Figure 8. Variations of compressive strength of cylinder specimens of mixing plans.

3.1. Slump test

This test was done based on the ASTM C143 (47) standard. The results of the slump test of all mixing plans, with a standard deviation of ±3 mm, are shown of Figure 7. According to this diagram, the slump is suitable in all plans and according to the standard.

3.2. Compressive strength test

The compressive strength test was performed on cylinder specimens with dimensions of 150 × 300 (diameter 150 mm, height 300 mm), similar to the ASTM C39 (48) standard. In this research, there are 10 mixing plans, the compressive strength of each plan is made from the average of three specimens. The results of the compressive strength of the mixing plans are given in Figure 8 and Table 8.

The results show that the replacement of rubber in concrete has reduced the strength of concrete. But the replacement of fine rubber has caused a further decrease in compressive strength. The compressive strength of the P10F5 plan has decreased by 27% due to the presence of fine aggregate rubber, and the P10B5 plan has decreased by 23% due to the presence of 5% glass crumb instead of fine concrete aggregate. The P10C5 plan, in which coarse rubber is replaced by coarse concrete aggregates, has a 11.5% reduction in compressive strength compared to the reference plan, which is probably due to the better granularity in terms of rubber size of this mixture compared to other mixing plans. These results are similar to previous research (38, 49, 50). The addition of micro-silica to concrete has increased the compressive strength, and this is due to the chemical effect of micro-silica as a highly reactive pozzolanic substance in concrete, as well as the physical effect of micro-silica in filling the voids between particles in concrete components (51, 52). As can be seen, the compressive strength of the P10C5M10 plan, which contains micro-silica, glass powder and coarse rubber, has increased by about 9% compared to the reference plan, and the compressive strength of the C5M10 plan, which contains micro-silica and coarse rubber, has the same compressive strength as the reference plan. Adding micro-silica to mixing plans with glass powder along with fine rubber and glass crumb has in-

Table 8. Compressive strength Variations compared to reference concrete.

Plan Symbol	Compressive Strength (MPa)	Compressive Strength Variations (%)
Reference	39	0
P10F5	28.5	-26.92
P10C5	34.5	-11.53
P10B5	30	-23.07
P10F5M10	36	-7.69
P10C5M10	42.5	+8.97
P10B5M10	37	-5.12
F5M10	35	-10.26
C5M10	39	0
B5M10	36	-7.69

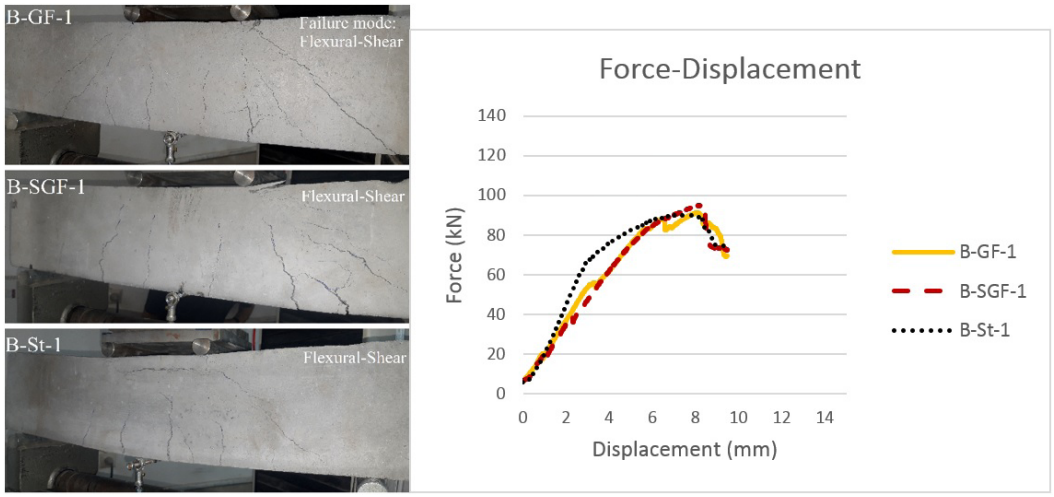

Figure 9. Beams reinforced with GFRP, SGFRP, and steel rebars with reference concrete under bending test.

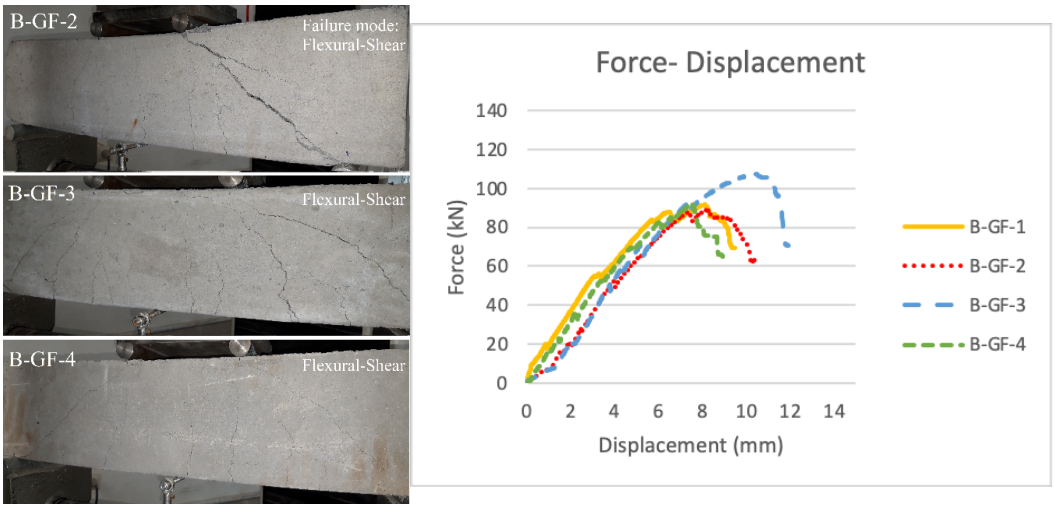

Figure 10. Beams reinforced with GFRP rebars with concrete mixing plans 2, 3, and 4 under bending test.

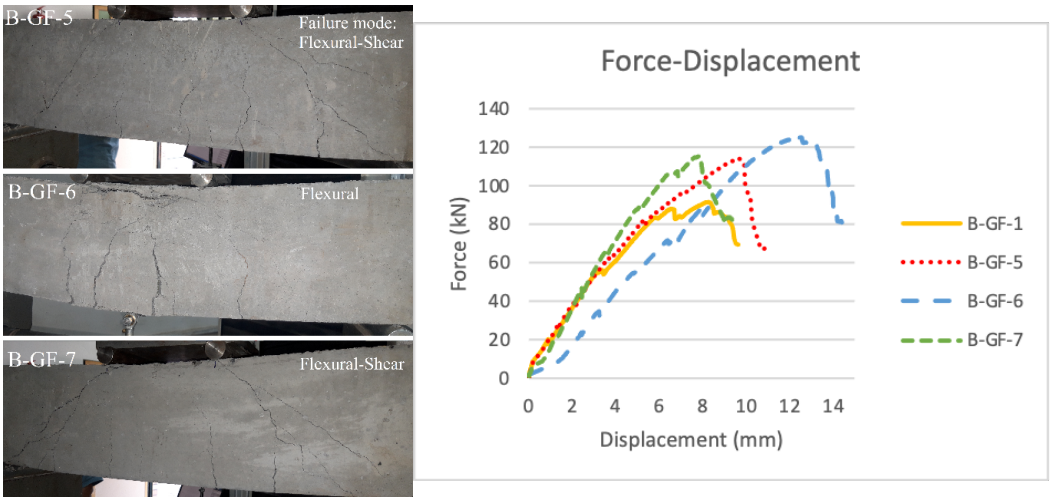

Figure 11. Beams reinforced with GFRP rebars with concrete mixing plans 5, 6, and 7 under bending test.

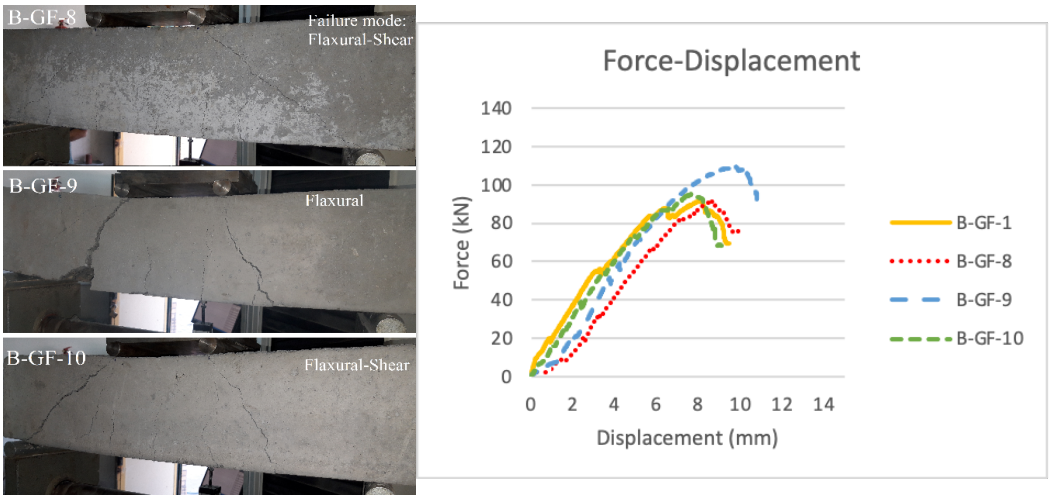

Figure 12. Beams reinforced with GFRP rebars with concrete mixing plans 8, 9, and 10 under bending test.

creased the compressive strength by 26%, and in the plan containing glass powder with coarse rubber has increased the compressive strength by 23%. The replacement effect of glass crumb was better than fine rubber in concrete, and this may be due to the less flexibility of glass crumb compared to fine rubber, or because of the presence of silica in glass crumb and its inclusion in the hydration reaction of concrete. By comparing similar mixing plans with glass powder and with micro-silica separately, it is clear that the replacement of micro-silica has a better effect and this can be due to the complete reaction of micro-silica in concrete compared to glass powder in the hydration process. In mixing plans containing rubber, the compressive strength is higher in all mixing plans containing coarse rubber than fine rubber. The weight of concrete with rubber and glass has decreased by about 2% compared to the reference concrete.

3.3. Bending strength test

Four-point bending test (three-point loading) was performed to determine the bending strength using a simple beam according to the ASTM C78 standard (53) on the specimens of the manufactured beams. LVDT (Linear Variable Differential Transformer) has been used to record the displacement under the beam. This test has been done on all beam specimens. The beams were loaded with two concentrated loads spaced 75 mm from the mid-span, creating a shear span of 200 mm on both sides. The specimens were loaded continuously and without shock. Loading was applied at a constant rate up to the breaking point. Loading was applied by displacement control at a speed of 1 mm/min.

3.3.1. Force-Displacement response

The results of the force displacement response of the bending strength test are shown in the form of four groups of different mixing plans and different rebars in Figures (9-12). For a better comparison of the results, B-GF-3 beam as a reference beam is placed in all figures. Fractures on the diagrams indicate the cracks created in the concrete during force and displacement increase. As it is clear in Figure 9, the bending behavior of all three beams is almost similar. The slope of the beam diagram reinforced with steel rebar is higher in the middle part. This could be due to the ductile behavior of steel rebar compared to GFRP rebar and similar behavior of steel rebar in the range between yield strength and ultimate strength. The corresponding displacement of ultimate force in all three rebars is close to each other. In Figure 10, the initial behavior of the beams is almost similar and they have the same slope. The B-GF-3 beam, which recorded a higher ultimate force in this group, has a greater displacement in failure force. This is due to the presence of glass powder and coarse rubber in the concrete of this beam. The amount of ultimate force in B-GF-2 and B-GF-4 beams are close to each other and they differ by about 3%, and it is similar to the B-GF-1 reference beam, but the failure in B-GF-4 beam happened earlier and had a higher force growth. According to Figure 11, B-GF-6 beam has recorded the highest ultimate force and displacement in all mixing plans, which shows the simultaneous effect of glass powder, coarse rubber and micro-silica in concrete. The slope of the beam diagram of B-GF-7 is slightly higher than the others, which is due to the presence of glass crumb in this mixing plan. The difference in ultimate force and displacement in B-GF-5 and B-GF-7 beams is about 6% and 23%, respectively, and shows the difference in the behavior of fine rubber and glass crumb in concrete. As can be seen of Figure 12, the B-GF-9 beam, whose concrete contains micro-silica and coarse rubber, has 19% and 15% more ultimate bending force than the B-GF-8 and B-GF-10 beams, respectively, and it is also 19% more compared to the

B-GF-1 reference beam. The upward slope of the diagrams is almost the same in all the beams, and the displacement of the B-GF-9 beam is more than all the beams, and the B-GF-10 beam is broken with less displacement. In comparing the replacement of glass powder and micro-silica to concrete mixtures with recycled materials, the effect of micro-silica has been 3% better on average. Of course, the maximum displacement in the ultimate bending force is greater in beams containing glass powder than micro-silica.

3.3.2. Ultimate bending force

The results of the bending force of the bending strength test are shown of Figure 13. According to this diagram, the B-SGF-1 beam reinforced with SGFRP rebar has a higher bending strength of 3.5% and 5.5%, respectively, than the B-GF-1 and B-St-1 beams with GFRP and steel rebars. This increase in bending strength compared to beam with GFRP rebar is due to the presence of sand on the surface of the rebar which creates greater adhesion and strength, and when compared to beam with steel rebar it is due to the higher ultimate tensile strength of SGFRP rebar. The B-GF-1 beam has a higher bending strength than the B-St-1 beam, and this is due to the higher ultimate tensile strength of the GFRP rebar compared to steel. The B-GF-3 beam has an 17.5% increase in bending strength compared to the reference beam with the same rebar (B-GF-1). This shows that the replacement of glass powder and coarse rubber in concrete has increased the bending strength, which is probably due to the tensile strength of replaced rubber and its proper adhesion to concrete, as well as the filling of small pores by glass powder that have not entered the reaction. The B-GF-2 beam also showed a 3% decrease and the B-GF-4 beam was equal to the reference beam in bending strength. Therefore, glass powder along with fine rubber reduces the bending strength and glass powder along with glass crumb does not reduce the bending strength compared to the reference beam. This could be due to the difference in the physical nature of fine rubber and glass crumb. Glass crumb have higher density and higher compressive strength than fine rubber. The hardness of glass crumb also causes more adhesion to concrete. By adding 10% of micro-silica to the mixing plans, there has been a great increase in bending strength and this is consistent with previous research (27, 30). This increase in bending strength in the B-GF-6 beam is 36% compared to the reference beam and 16% compared to the B-GF-3 beam, which contains the same plan without micro-silica. B-GF-5 and B-GF-7 beams showed a 28% and 25% increase in bending strength, respectively, compared to B-GF-2 and B-GF-4 beams, which are similar to the same mixing plans but without micro-silica. The replacement of micro-silica due to the physical and chemical effects mentioned and coarse rubber due to its elastic nature and shape, along with glass powder in concrete, has increased the bending strength. The replacement of micro-silica in mixing plans without glass powder has increased the bending strength. Compared to the reference beam, the B-GF-9 beam shows an increase of 18.5% and the B-GF-10 beam also indicates an increase of about 3.5% in bending strength. The B-GF-8 beam, which contains fine rubber and micro-silica, had the same bending strength as the reference beam.

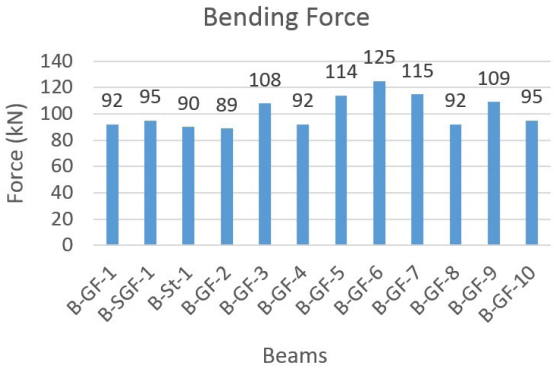

Figure 13. Ultimate bending force in the tested beams.

3.3.3. Failure mode

In general, the cracks are formed in the bending region of the beam and after the force exceeds the tensile strength of concrete. These cracks expand and propagate upward with increasing load. Next, with increasing load, new cracks are created in the shear zone.

The cracks of beams with normal concrete were initially bending, and after reaching the ultimate force and increasing displacement, they appeared in shear. The propagation of cracks in beams containing coarse rubber is seen more uniformly. The width of the cracks at the ultimate force was smaller in the beams containing rubber, and the bending behavior of the beams containing coarse rubber was better. It can be said that the presence of rubber, especially coarse rubber, in concrete acts as fasteners with different thicknesses that are distributed in the beam sections and reduce the width of the cracks. In the beams containing glass crumb, the shear cracks appear with greater length and width. In general, by applying force to the beams, bending cracks were first created, and with increasing force and displacement, shear cracks appeared and spread in the beams.

3.3.4. Ductility

Ductile materials are materials that can withstand loads in high strains. For reinforced concrete members, ductility is the load-carrying ability to undergo large inelastic deformations before the member fails.

On the other hand, the combination of fully elastic tensile behavior of FRP rebars along with the brittle performance of concrete creates a member lacking ductility with brittle failure. One approach to compensate the ductility of reinforced concrete beams with FRP reinforcements is to add or replace materials such as rubber to concrete.

The highest displacement in ultimate force in concrete beams is related to beams containing coarse rubber. The displacement of B-GF-3, B-GF-6, and B-GF-9 beams, which all have coarse rubber, was 29%, 54%, and 21% higher than the reference beam B-GF-1, respectively. Beams containing fine rubber had more displacement than the reference beams, so it showed an increase of 19% in the B-GF-5 beam. These results are also consistent with previous research (24, 26). Adding or replacing elastic materials such as rubber to concrete creates non-brittle and flexible concrete. The reason for the increased ductility in these beams can be the flexibility of the rubber itself when applying force and its proper tensile capacity before separating from the surrounding concrete. The replacement of micro-silica in similar mixtures has increased displacement, and its highest amount is in beam B-GF-6 with an increase of 19.5%. The displacements of beams containing glass crumb were also similar and on average were about 6% less than the reference beam B-GF-1. The inflexibility of glass crumb, which is a brittle material, has reduced displacement.

In general, the addition of glass powder and micro-silica to mixtures containing recycled rubber has helped to improve ductility. The displacement of the center of the span in the ultimate force of the tested beams is shown of Figure 14.

3.3.5. Modulus of Rupture

When an element is subjected to bending stress, it applies both tensile and bending forces to an element. This issue leads to uneven distribution of forces among its fibers. The fibers that are at the surface of the element bear the most forces, as a result, they are subject to failure or breakage more than other fibers.

Calculation of modulus of rupture is very important in structural mechanics. This index improves the design of structural elements such as beams, flexural members, shafts, etc. This index helps to know the materials and their characteristics and also predicts the resistance and stability of the elements. This modulus is affected by mixing ratios, size and amount of aggregate used and other factors of sample making.

The modulus of rupture is calculated using the results of the bending test based on the ASTM C78 standard and according to the loading conditions and the fracture position on the tensile surface of the beam, based on Equation [1]:

$$R = \frac{3Pa}{bd^2} \qquad [1]$$

where:

R = modulus of rupture, MPa,

P = maximum applied force indicated by the testing machine, N,

b = average width of specimen, mm, at the fracture,

d = average depth of specimen, mm,

a = average distance between line of fracture and the nearest support measured on the tension surface of the beam, mm.

The results obtained for the modulus of rupture in the tested beams are shown in Figure 15. The results show that the highest modulus of rupture is related to the B-GF-6 beam, which contains glass powder and micro-silica along with coarse rubber, and it is about 36% higher than the similar reference beam. Considering the effect of the type of aggregates and materials used in concrete on the modulus of rupture, the presence of coarse rubber with high tensile strength, as well as the effect of glass powder and micro-silica in increasing the compressive strength and bending strength of concrete, can be factors in increasing the modulus of rupture in this beam. The lowest one is related to the beam with GFRP rebar with concrete containing fine rubber and glass powder, which has a dif-

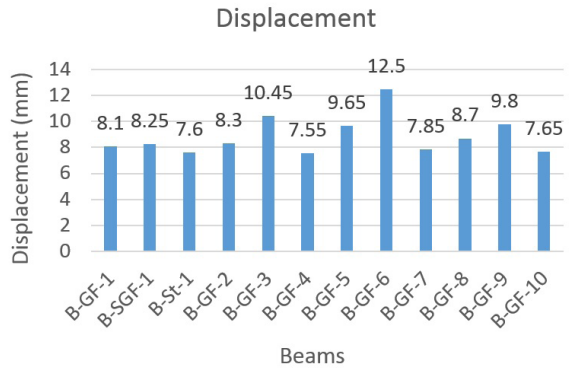

Figure 14. Displacement of beams under bending test.

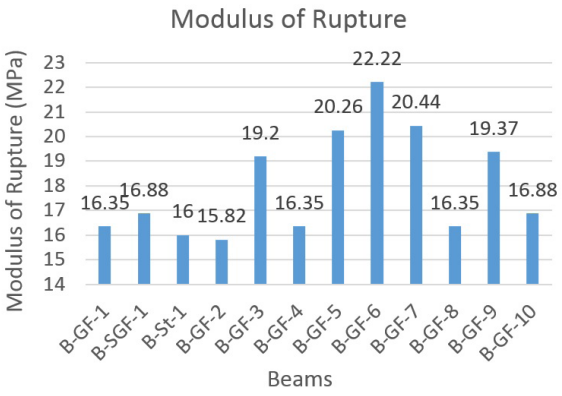

Figure 15. Modulus of rupture of beams.

ference of 2% compared to the similar reference beam. This can be due to the lower adhesive surface of fine rubber to concrete and the lower tensile and compressive strength of concrete made from it compared to coarse rubber. In the beams that contain glass crumb, the B-GF-7 beam has the highest modulus of rupture, which is about 25% higher than the similar reference concrete. In the beams with fine rubber composition, the B-GF-5 beam has the highest modulus of rupture, which is about 23% higher than the similar reference concrete. In both the latter cases, this increase is due to the presence of micro-silica and glass powder in their concrete mixing plans and their effect in increasing the bending strength of the beams.

3.3.6. Comparison of three-point bending test and four-point bending test of beams with composite rebars

In this section, a three-point bending test (center-point loading) was performed to determine the bending strength of a simple beam according to the ASTM C293 standard (54). LVDT was used to record the displacement under the beam. As shown in Figure 16, this beam is loaded with a force in the middle of the span and creates a shear span of 275 mm on each side. The force application conditions and loading speed were completely similar to the four-point bending test. This test was performed on one of the beams made with reference concrete and reinforced with SGFRP rebar (B-SGF-1-2) and compared with the same specimen under the four-point bending test (B-SGF-1). The results showed that the ultimate bending force in the beam in three-point bending test was 6% more than the four-point bending test. The amount of displacement in the ultimate bending force was also 23% higher. The behavior of this beam was completely bending and no shear cracks were seen in it. As the force increased, a crack first appeared in the middle of the beam and then extended upwards. The width and depth of the crack increased until the rupture occurred. The results of both bending test are shown of Figure 17.

3.4. Evaluation of beams with FRP rebars after bending loading

As it is clear in Figure 18, the GFRP rebar is a rupture in this part of the concrete, and the separation or pulling out of the rebar from the concrete is not seen. Therefore, it can be concluded that the adhesion on the surface of GFRP rebar and concrete is suitable. Another point of this Figure is the shear failure of the GFRP rebar, which clearly shows the weakness of these rebars.

Figure 19 shows the specimen of the concrete beam with SGFRP rebar under bending test. As can be seen, the sand coating remains on the rebar. Adhesion of SGFRP rebar surface to concrete is suitable and pulling out of the rebar from inside the concrete is not observed. In general, the performance of SGFRP rebar is better than GFRP rebar.

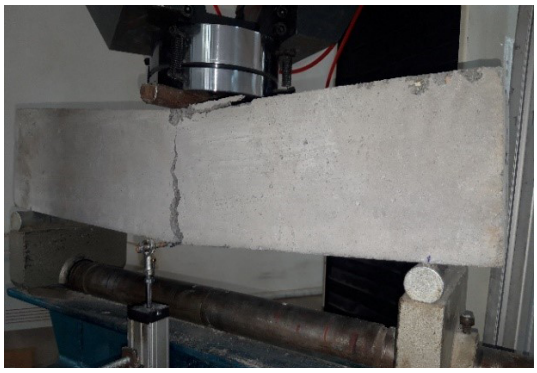

Figure 16. Beam specimen under three-point bending test.

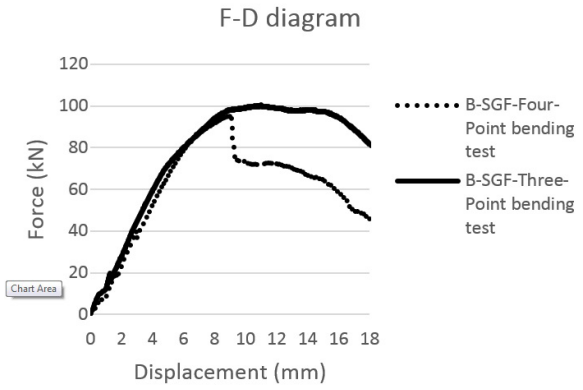

Figure 17. Force-Displacement curve of three-point bending test and four-point bending test rebars.

3.5. Scanning Electron Microscope (SEM) images

Scanning electron microscope imaging was done to investigate the microstructure characteristics of concrete. Figure 20 shows microscopic images of normal concrete specimens, concrete with fine rubber and coarse rubber, respectively.

Calcium silicate hydrate (C-S-H) is the main adhesive in cement and concrete made from it, and it starts to form from the initial stages of cement hydration, and gradually the cement becomes dense. In Figure 20 (a), hydration products such as C-S-H gel and calcium hydroxide (C-H) crystals in concrete can be seen. Concrete in this part has a homogeneous texture and no large holes are observed in it. In a part of concrete, needle-shaped ettringite crystals are also seen. Ettringite is the mineral name for calcium sulfoaluminate which is commonly found in Portland cement concrete. Sources of calcium sulfate, such as gypsum, are intentionally added to Portland cement to moderate initial hydration reactions to prevent rapid setting. Figure 20 (b) shows that the adhe-

Figure 18. Rupture of GFRP rebar in concrete beam after loading.

Figure 19. SGFRP rebar in concrete beam after loading.

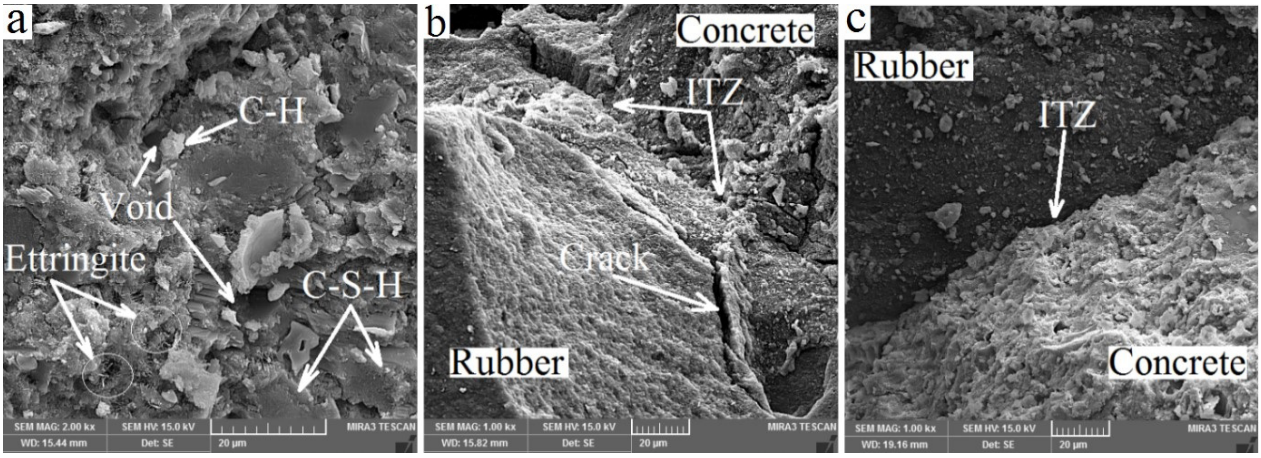

Figure 20. SEM images of microstructure a) Normal concrete b) Concrete containing fine rubber and glass powder c) Concrete containing coarse rubber and glass powder.

sion between fine rubber and concrete is suitable, but in some parts, cracks caused by the application of force can be seen. These cracks occurred in two areas. One in the rubber itself and the other in the transfer surface between

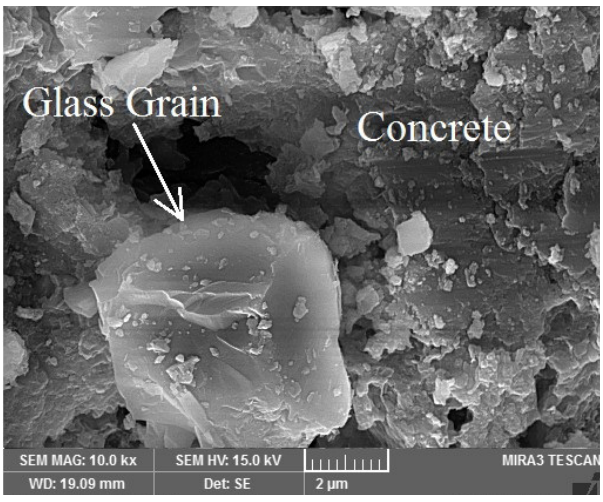

Figure 21. Glass grain in concrete.

the rubber and the concrete adhesive. Of course, in fine rubber, separation occurred more in the Interfacial Transition Zone (ITZ). Figure 20 (c) also shows good adhesion between coarse rubber and concrete. The texture of the concrete in this part is very uniform and large holes and porosity are not seen. In specimens with coarse rubber, the adhesion of rubber and concrete mortar was better after applying force.

The image of the glass grain in the concrete that has not yet fully reacted is shown in Figure 21. Part of the glass powder and silica in it reacts in the long term and increases the concrete strength.

4. CONCLUSIONS

In this research, the bending behavior of reinforced concrete beams containing recycled glass, rubber and micro-silica with composite rebars (GFRP, SGFRP) and steel rebar has been investigated. Concrete beams with different mixing plans and rebars were made and then subjected to four-point bending test. The investigated variables included the type of rebar, the size of the replacement rubber, the size of the replacement glass, and the type of combination of glass, rubber, and micro-silica. The effects of these variable on the force-deformation behavior, crack pattern, modulus of rupture, and ductility of the beam specimens were investigated. Investigating the microstructure characteristics of concrete containing recycled materials has been done by scanning electron microscope imaging (SEM).

The general results of the research are as follows:

- The larger the size of the replacement rubber (5-10 mm), the more effective it will be in reducing the workability of concrete.
- In general, adding glass powder with rubber with dimensions of 5 to 10 mm has reduced the compressive strength less than rubber with dimensions of 0 to 5 mm, and adding micro-silica to these mixing plans increases the compressive strength even more than the reference concrete.
- Beams reinforced with GFRP and SGFRP composite rebars showed higher bending strength than steel rebars.
- It can be concluded that adding glass powder and coarse rubber to concrete increases the bending strength by 17.5%.
- Substituting micro-silica in mixing plans with glass powder has greatly increased the bending strength. Substituting micro-silica in mixing plans containing rubber compensates for the reduction in strength due to the presence of rubber. The effect of micro-silica replacement was slightly better compared to glass powder in similar mixing plans.
- Substitution of glass powder and rubber, especially coarse rubber in concrete mixtures, causes more displacement in the ultimate bending force in beams under bending, which increases to 29% in the best cases. The replacement of micro-silica in similar mixtures increases the ductility and the highest amount of this increase is 19.5%. Replacing glass crumb instead of sand in concrete reduces ductility by about 28%.
- The low shear strength of FRP rebars, which is one of the weak points of these rebars, was lower in beams reinforced by sand-blasted rebars.
- In general, addition or replacement of materials such as rubber and glass in the concrete mix can increase the ultimate bending capacity and displacement, and these provide more warning before failure.
- The highest modulus of rupture has been recorded in the mixing plans that include glass powder and micro-silica. Its highest value has an increase of 36% compared to the reference concrete beam.
- In general, in the survey of concrete microstructure, the adhesion of rubber and concrete surface was suitable. In concretes containing fine rubber, breakage and separation of the rubber can be seen. In the concretes containing coarse rubber, there were more fractures in the rubber itself, which can be one of the reasons for the increased bending strength of these specimens.

Declaration of conflict of interest

The authors declare that there is no conflict of interest.

AUTHOR CONTRIBUTIONS:

Conceptualization: R. Jafari, M.H. Alizadeh Elizei, M. Ziaei, R. Esmaeil Abadi. Data cleansing: R. Jafari, M. Ziaei. Formal analysis: R. Jafari, M.H. Alizadeh Elizei, M. Ziaei. Research: R. Jafari, M. Ziaei. Methodology: R. Jafari, M.H. Alizadeh Elizei, M. Ziaei, R. Esmaeil Abadi. Project administration: R. Jafari, M.H. Alizadeh Elizei. Resources: R. Jafari, M. Ziaei. Supervision: M. Ziaei, R. Esmaeil Abadi. Validation: R. Jafari, M.H. Alizadeh Elizei, M. Ziaei, R. Esmaeil Abadi. Visualization: R. Jafari. Writing, original draft: R. Jafari. Writing, review and editing: R. Jafari, M.H. Alizadeh Elizei, M. Ziaei, R. Esmaeil Abadi.

REFERENCES

1. Hosseini, S.M.; Mostofinejad, D. (2021) Seismic performance of RC short columns retrofitted with a novel system in shear and flexure using CFRP composites. *J. Compos. Constr.* 25 [5]. https://doi.org/10.1061/(ASCE)CC.1943-5614.0001148.
2. Ali, O.; Bigaud, D.; Riahi, H.S. (2018) Seismic performance of reinforced concrete frame structures strengthened with FRP laminates using a reliability-based advanced approach. *Compos. B. Eng.* 139, 238-248. https://doi.org/10.1016/j.compositesb.2017.11.051.
3. Hadigheh, S.A.; Mahini, S.S.; Maheri, M.R. (2014) Seismic behavior of FRP-Retrofitted reinforced concrete frames. *J. Earthq. Eng.* 18 [8], 1171-1197. https://doi.org/10.1080/13632469.2014.926301.
4. Attari, N.; Youcef, Y.S.; Amziane, S. (2019) Seismic performance of reinforced concrete beam–column joint

strengthening by frp sheets. *Struct*. 20, 353-364. https://doi.org/10.1016/j.istruc.2019.04.007.
5. Schützenhofer, S.; Kovacic, I.; Rechberger, H.; Mack, S. (2022) Improvement of environmental sustainability and circular economy through construction waste management for material reuse. *Sustain*. 14 [17], 11087. https://doi.org/10.3390/su141711087.
6. Lamba, P.; Kaur, D.P.; Raj, S.; Sorout, J. (2022) Recycling/reuse of plastic waste as construction material for sustainable development: a review. *Environ. Sci. Pollut. Res.* 29, 86156–86179. https://doi.org/10.1007/s11356-021-16980-y.
7. Terro, M. (2006) Properties of concrete made with recycled crushed glass at elevated temperatures. *Build. Environ*. 41 [5], 633–639. https://doi.org/10.1016/j.buildenv.2005.02.018.
8. Youssf, O.; Hassanli, R.; Mills, J.E.; Skinner, W.; Ma, X.; Zhuge, Y.; Roychand, R.; Gravina, R. (2019) Influence of mixing procedures, rubber treatment, and fibre additives on rubcrete performance. *J. Compos. Scien*. 3 [2], 41. https://doi.org/10.3390/jcs3020041.
9. Hassanli, R.; Youssf, O.; Mills, J.E. (2017) Experimental investigations of reinforced rubberised concrete structural members. *J. Build. Eng*. 10, 149–165. https://doi.org/10.1016/j.jobe.2017.03.006.
10. Al-Tayeb, M.M.; Bakar, B.A.; Ismail, H.; Akil, H.M. (2013) Effect of partial replacement of sand by recycled fine crumb rubber on the performance of hybrid rubberised -normal concrete under impact load: Experiment and simulation. *J. Clean. Prod.* 59, 284–289.
11. Youssf, O.; ElGawady, M.A.; Mills, J.E. (2015) Experimental investigation of crumb rubber concrete columns under seismic loading. *Struct*. 3, 13–27. https://doi.org/10.1016/j.istruc.2015.02.005.
12. Youssf, O.; ElGawady, M.A.; Mills, J.E. (2016) Static cyclic behaviour of FRP-confined crumb rubber concrete columns. *Eng. Struct*. 113, 371–387. https://doi.org/10.1016/j.engstruct.2016.01.033.
13. Murad, Y.; Tarawneh, A.; Arar, F.; Al-Zu'bi, A.; Al-Ghwairi, A.; Al-Jaafreh, A.; Tarawneh, M. (2021) Flexural strength prediction for concrete beams reinforced with FRP bars using gene expression programming. *Struct*. 33, 3163-3172. https://doi.org/10.1016/j.istruc.2021.06.045.
14. Falah Hassan, H.; Kadhim Medhlom, M.; Sinan Ahmed, A.; Husein Al-Dahlaki, M. (2020) Flexural performance of concrete beams reinforced by GFRP bars and strengthened by CFRP sheets. *Case Stud. Constr. Mater.* 13, e00417. https://doi.org/10.1016/j.cscm.2020.e00417.
15. Al-Sunna, R.; Pilakoutas, K.; Hajirasouliha, I.; Guadagnini, M. (2012) Deflection behaviour of FRP reinforced concrete beams and slabs: an experimental investigation. *Compos. B. Eng*. 43 [5], 2125–2134. https://doi.org/10.1016/j.compositesb.2012.03.007.
16. Yang, J.M.; Min, K.H.; Shin, H.O.; Yoon, Y.S. (2012) Effect of steel and synthetic fibers on flexural behavior of high-strength concrete beams reinforced with FRP bars. *Compos. B. Eng.* 43 [3], 1077–1086. https://doi.org/10.1016/j.compositesb.2012.01.044.
17. El-Nemr, A.; Ahmed, E.A.; Benmokrane, B. (2013) Flexural behavior and serviceability of normal-and high-strength concrete beams reinforced with glass fiber-reinforced polymer bars. *ACI. Struct. J.* 110 [6], 1077. Retrieved from https://www.researchgate.net/publication/256287944.
18. Yoo, D.Y.; Banthia, N.; Yoon, Y.S. (2016) Flexural behavior of ultra-high-performance fiber reinforced concrete beams reinforced with GFRP and steel rebars. *Eng. Struct.* 111, 246–262. https://doi.org/10.1016/j.engstruct.2015.12.003.
19. El-Nemr, A.; Ahmed, E.A.; Barris, C.; Benmokrane, B. (2016) Bond-dependent coeffcient of glass-and carbon-FRP bars in normal-and high-strength concretes. *Constr. Build. Mater.* 113, 77–89. https://doi.org/10.1016/j.conbuildmat.2016.03.005.
20. Rahman, S.H.; Mahmoud, K.; El-Salakawy, E. (2016) Behavior of glass fiber-reinforced polymer reinforced concrete continuous T-beams. *J. Compos. Constr*. 21 [2], 04016085. https://doi.org/10.1061/(ASCE)CC.1943-5614.0000740.
21. Duic, J.; Kenno, S.; Das, S. (2018) Performance of concrete beams reinforced with basalt fibre composite rebar. *Constr. Build. Mater.* 176, 470–481. https://doi.org/10.1016/j.conbuildmat.2018.04.208.
22. Abdelkarim, O.I.; Ahmed, E.A.; Mohamed, H.M.; Benmokrane, B. (2019) Flexural strength and serviceability evaluation of concrete beams reinforced with deformed GFRP bars. *Eng. Struct*. 186, 282–296. https://doi.org/10.1016/j.engstruct.2019.02.024.
23. Hama, S.M.; Mahmoud, A.S.; Yassen, M.M. (2019) Flexural behavior of reinforced concrete beam incorporating waste glass powder. *Struct.* 20, 510-518. https://doi.org/10.1016/j.istruc.2019.05.012.
24. Eisa, A.S.; Elshazli, M.T.; Nawar, M.T. (2020) Experimental investigation on the effect of using crumb rubber and steel fibers on the structural behavior of reinforced concrete beams. 252, 119078. *Constr. Buid. Mater.* https://doi.org/10.1016/j.conbuildmat.2020.119078.
25. Shahjalal, M.D.; Islam, K.; Rahman, J.; Ahmed, K.S.; Karim, M.R.; Billah, A.M. (2021) Flexural response of fiber reinforced concrete beams with waste tires rubber and recycled aggregate. 278, 123842. *J. Clean. Prod*. https://doi.org/10.1016/j.jclepro.2020.123842.
26. Ismail, M.K.; Hassan, A.A.A. (2017) An experimental study on flexural behaviour of large-scale concrete beams incorporating crumb rubber and steel fibres. *j. Eng. Struct.* 145, 97-108. http://doi.org/10.1016/j.engstruct.2017.05.018.
27. Erfan, A.M.; Hassan, H.E.; Khalil, M.H.; El-Sayed, T.A. (2020) The flexural behavior of nano concrete and high strength concrete usingGFRP. *Constr. Build. Mater*. 247, 1188664. https://doi.org/10.1016/j.conbuildmat.2020.118664.
28. De Sá, F.R.G.; Silva, F.d.A.; Cardoso, D.C.T. (2020) Tensile and flexural performance of concrete members reinforced with polypropylene fibers and GFRP bars. *Compos. Struct*. 253, 112784. https://doi.org/10.1016/j.compstruct.2020.112784.
29. Arunbalaji, G.; Nanthakumar, N.; Suganya, R. (2017) Behaviour of reinforced concrete beam containing micro-silica and nano-silica. *Int. J. Eng. Technol*. 48 [3], 140-146. https://doi.org/10.14445/22315381/IJETT-V48P225.
30. El-Mandouh, M.A.; Kaloop, M.R.; Hu, J.W.; Abd El-Maula, A.S. (2022) Shear strength of nano-silica high-strength reinforced concrete beams. *Mater*. 15 [11], 3755. https://doi.org/10.3390/ma15113755.
31. Jafari, R.; Alizadeh Elizei, M.H.; Ziaei, M.; Esmaeil Abadi, R. (2022) Laboratory study of mechanical performance of concrete containing waste glass and rubber at high temperature. *Modar. Civ. Eng. J*. 23 [1], 179-192. https://doi.org/10.22034/23.1.12.
32. Sadiqul Islam, G.M.; Rahman, M.H.; Kazi, M. (2017) Waste glass powder as partial replacement of cement for sustainable concrete practice. *Int. J. Sustain. Built Environ*. 6 [1], 37-44. https://doi.org/10.1016/j.ijsbe.2016.10.005.
33. Gupta, T.; Chaudhary, S.; Sharma, A.K. (2015) Mechanical and durability properties of waste rubber fiber concrete with and without silica fume. *J. Clean. Prod*. 112 [1], 702-711. http://doi.org/10.1016/j.jclepro.2015.07.081.
34. Iranian Concrete Code (ABA) - Second revision, (1400), Department of technical and executive affairs of the country, Plan and Budget Organization, Iran.
35. ASTM C128-22 (2022). Standard test method for relative density (specific gravity) and absorption of fine aggregate. American Society for Testing and Materials (ASTM). https://doi.org/10.1520/C0128-22.
36. ASTM C127-15 (2015). Standard test method for relative density (specific gravity) and absorption of coarse aggregate. American Society for Testing and Materials (ASTM). https://doi.org/10.1520/C0127-15.
37. ASTM C150-22 (2022). Standard specification for portland cement. american society for testing and materials. American Society for Testing and Materials (ASTM). https://doi.org/10.1520/C0150_C0150M-22.
38. Sgobba, S.; Borsa, M.; Molfetta, M.; Carlo Marano, G. (2015) Mechanical performance and medium-term degradation of rubberized concrete. *Constr. Build. Mater*. 98, 820–831. https://doi.org/10.1016/j.conbuildmat.2015.07.095.
39. Kiani Oskooi, R.; Maleki, A. (2018) Investigation of the effect of glass powder waste with different granulation of stone materials on concrete strength. *Tabriz, Confer.Civ. Eng.* 1397, 1.

40. ASTM C1240-20 (2020). Standard specification for silica fume used in cementitious mixtures. American Society for Testing and Materials (ASTM). https://doi.org/10.1520/C1240-20.
41. ACI-211.1-91. Standard practice for selecting proportions for normal, heavy weight, and, mas concrete. American Concrete Institute (ACI).
42. ACI 440.1R15. (2015). Guide for the plan and construction of concrete reinforced with FRP bars. Farmington Hills. Michigan.
43. ACI 318-19 (2019). Building code requirements for structural concrete. American Concrete Institute (ACI).
44. ASTM C192/C192M-19 (2019). Standard practice for making and curing concrete test specimens in the laboratory. American Society for Testing and Materials (ASTM). https://doi.org/10.1520/C0192_C0192M-19.
45. ASTM C172/C172M-17 (2017). Standard practice for sampling freshly mixed concrete. American Society for Testing and Materials (ASTM). https://doi.org/10.1520/C0172_C0172M-17.
46. ASTM C511-21 (2021). Standard specification for mixing rooms, moist cabinets, moist rooms, and water storage tanks used in the testing of hydraulic cements and concretes. American Society for Testing and Materials (ASTM). https://doi.org/10.1520/C0511-21.
47. ASTM C143/C143M-20 (2020). Standard test method for slump of hydraulic-cement concrete. American Society for Testing and Materials (ASTM). https://doi.org/10.1520/C0143_C0143M-20.
48. ASTM C39/C39M−21 (2021). Standard test method for compressive strength of cylindrical concrete specimens. American Society for Testing and Materials (ASTM). https://doi.org/10.1520/C0039_C0039M-21.
49. Ganjian, E.; Khorami, M.; Maghsoudi, A. (2009) Scrap-tyre-rubber replacement for aggregate and filler in concrete. *Constr. Build. Mater*. 23, [5], 1828–1836. https://doi.org/10.1016/j.conbuildmat.2008.09.020.
50. Pacheco-Torgal, F.; Ding, Y.; Jalali, S. (2012) Properties and durability of concrete containing polymeric wastes (tyre rubber and polyethylene terephthalate bottles): An overview. *Constr. Build. Mater*. 30, 714-724. https://doi.org/10.1016/j.conbuildmat.2011.11.047.
51. Güneyisi, E.; Gesoglu, M.; Ozturan, T. (2004) Properties of rubberized concretes containing silica fume. *Cem. Concr. Res*. 34 [12], 2309-2317. https://doi.org/10.1016/j.cemconres.2004.04.005.
52. Gesoglu, M.; Guneyisi, E. (2007) Strength development and chloride penetration in rubberized concrete with and without rubberized silica fume. *Mater. Struct*. 40, 953-964. https://doi.org/10.1617/s11527-007-9279-0.
53. ASTM C78/C78M−22 (2022). Standard test method for flexural strength of concrete (using simple beam with third-point loading). American Society for Testing and Materials (ASTM). https://doi.org/10.1520/C0078_C0078M-22.
54. ASTM C293/C293M−16 (2016). Standard test method for flexural strength of concrete (using simple beam with center-point loading). American Society for Testing and Materials (ASTM). https://doi.org/10.1520/C0293_C0293M-16.